Dual Ablation of Grb10 and Grb14 in Mice Reveals Their Combined Role in Regulation of Insulin Signaling and Glucose Homeostasis

Lowenna J. Holt, Ruth J. Lyons, Ashleigh S. Ryan, Susan M. Beale, Andrew Ward, Gregory J. Cooney,* and Roger J. Daly*

Cancer Research Program (L.J.H., R.J.L., A.S.R., R.J.D.) and Diabetes and Obesity Research Program (S.M.B., G.J.C.), Garvan Institute of Medical Research, Darlinghurst, Sydney, New South Wales 2010, Australia; and Department of Biology and Biochemistry (A.W.), University of Bath, Claverton Down, Bath BA2 7AY, United Kingdom

Growth factor receptor bound (Grb)10 and Grb14 are closely related adaptor proteins that bind directly to the insulin receptor (IR) and regulate insulin-induced IR tyrosine phosphorylation and signaling to IRS-1 and Akt. Grb10- and Grb14-deficient mice both exhibit improved whole-body glucose homeostasis as a consequence of enhanced insulin signaling and, in the case of the former, altered body composition. However, the combined physiological role of these adaptors has remained undefined. In this study we utilize compound gene knockout mice to demonstrate that although deficiency in one adaptor can enhance insulin-induced IRS-1 phosphorylation and Akt activation, insulin signaling is not increased further upon dual ablation of Grb10 and Grb14. Context-dependent limiting mechanisms appear to include IR hypophosphorylation and decreased IRS-1 expression. In addition, the compound knockouts exhibit an increase in lean mass comparable to Grb10-deficient mice, indicating that this reflects a regulatory function specific to Grb10. However, despite the absence of additive effects on insulin signaling and body composition, the double-knockout mice are protected from the impaired glucose tolerance that results from high-fat feeding, whereas protection is not observed with animals deficient for individual adaptors. These results indicate that, in addition to their described effects on IRS-1/Akt, Grb10 and Grb14 may regulate whole-body glucose homeostasis by additional mechanisms and highlight these adaptors as potential therapeutic targets for amelioration of the insulin resistance associated with type 2 diabetes. **(*Molecular Endocrinology* 23: 1406–1414, 2009)**

The hormone insulin is preeminent for the regulation of whole-body glucose homeostasis and mediates its cellular responses in target tissues by binding to the insulin receptor (IR). Insulin-induced receptor activation triggers intracellular signaling cascades that promote glucose uptake into muscle and fat, inhibit hepatic glucose production, and enhance lipogenesis, as well as glycogen and protein synthesis (1). The development of insulin resistance in muscle, which can be due to genetic factors, a sedentary lifestyle, ageing, and/or obesity, is a major risk factor for development of type 2 diabetes. Although the pancreatic β-cells initially compensate by producing more insulin, β-cell failure eventually occurs, leading to glucose intolerance and overt diabetes (2).

The IR and its downstream targets, insulin receptor substrates (IRS)-1 and IRS-2, constitute a critical node in the insulin-signaling network (3). Tyrosine phosphorylation of IRS proteins generates binding sites for a variety of src homology (SH)2 domain-containing proteins including growth factor receptor-bound (Grb)2 and the p85 subunit of phosphatidylinositol (PI) 3-kinase. The latter enzyme plays a pivotal role in mediating metabolic re-

ISSN Print 0888-8809 ISSN Online 1944-9917
Printed in U.S.A.

doi: 10.1210/me.2008-0386 Received October 13, 2008. Accepted June 8, 2009.
First Published Online June 18, 2009
* G.J.C. and R.J.D. are joint senior authors.

Abbreviations: BPS, Between pleckstrin homology and SH2; dKO, double-knockout OΔ2-4$^{m/+}$; DXA, dual-energy x-ray absorptiometry; Grb, growth factor receptor-bound; HFD, high-fat diet; IR, insulin receptor; IRS, insulin receptor substrate; PI, phosphatidylinositol; PLSD, protected least significant difference; PTP, protein tyrosine phosphatase; WT, wild type.

sponses to insulin, including glucose transporter 4 translocation to the plasma membrane and glycogen synthesis, and a key PI 3-kinase effector implicated in regulation of these endpoints is the serine/threonine kinase Akt (3). Signal transmission downstream of the IR is regulated at different steps by specific protein and lipid phosphatases, adaptors and E3 ubiquitin ligases, and some of these represent potential therapeutic targets for amelioration of insulin resistance (3, 4). For example, IR tyrosine phosphorylation is negatively regulated by protein tyrosine phosphatase (PTP)1b (5), and treatment of diabetic ob/ob mice with PTP1b-directed antisense oligonucleotides leads to enhanced IR phosphorylation and downstream signaling (6).

Grb10 and Grb14 are members of a family of SH2-containing adaptors that also includes Grb7 (7, 8). Both Grb10 and Grb14 bind directly to the insulin receptor (IR) via two regions: the between pleckstrin homology and SH2 (BPS) domain, and the SH2 domain (8, 9). In terms of function and underlying mechanism, Grb14 is the best-characterized of these two adaptors. Grb14-deficient mice exhibit improved glucose homeostasis, despite lower circulating insulin levels, and enhanced insulin signaling via IRS-1 and Akt in liver and skeletal muscle (10). Structural studies have revealed how Grb14 regulates IR signal output, identifying the N-terminal region of the Grb14 BPS domain as a pseudosubstrate inhibitor of the IR kinase (9). An additional effect observed in Grb14-deficient animals is that the liver IR is relatively hypophosphorylated upon insulin stimulation, which appears to reflect a role for Grb14 in protecting the IR activation loop from the action of specific protein tyrosine phosphatases (10–12). Interestingly, Grb14 expression is increased in adipose tissue of insulin-resistant animal models and type 2 diabetic human patients (13), suggesting that Grb14 may modulate insulin sensitivity in pathological, as well as in normal, states.

Grb10-deficient mice exhibit enhanced insulin-induced tyrosine phosphorylation of IRS-1, and associated IR hypophosphorylation, in muscle and white adipose tissue (14). The gene-disrupted mice also exhibit improved whole-body glucose homeostasis and insulin sensitivity, which reflects a modest enhancement of insulin action in skeletal muscle and adipose tissue, together with a significant increase in skeletal muscle mass (14). Consistent with these data, a different strain of Grb10 gene knockout mice exhibit enhanced insulin-induced activation of Akt and Erk in skeletal muscle and adipose tissue and increased insulin sensitivity in skeletal muscle (15).

Comparison of the respective gene knockouts suggests that Grb10 and Grb14 exhibit partially overlapping functions *in vivo*. To formally define the combined physiological roles of Grb10 and Grb14, we have generated and characterized compound gene knockout mice deficient for both proteins. This provides further insights into the roles of these adaptors in regulating insulin signaling in particular tissues and, importantly, identifies that ablation of both proteins protects against the impaired glucose tolerance that results from high-fat feeding.

Results

Effect of compound Grb10 and Grb14 gene disruption on body weight and body composition

We bred Grb10 heterozygote mice, on a mixed C57BL/6:CBA background, with Grb14 heterozygote mice, on a C57BL/6 background, to generate single and compound deletions for these genes. Due to reduced fertility of Grb10 gene-disrupted females, it was difficult to establish a colony of mice that were homozygous for the Grb10 deletion. Because Grb10 is an imprinted gene, disruption of the maternal allele ablates Grb10 expression in peripheral tissues (16). Therefore, we used these maternal heterozygotes (denoted Grb10Δ2–4$^{m/+}$) for the current study. The genotype of the compound deletion was Grb10Δ2-4$^{m/+}$Grb14$^{-/-}$, denoted henceforth as dKOΔ2-4$^{m/+}$. To confirm ablation of these adaptors in dKOΔ2-4$^{m/+}$ animals, Western blot analysis was undertaken on white adipose tissue and liver, tissues that express high levels of Grb10 and Grb14, respectively (10, 15). This confirmed absence of protein expression (Fig. 1).

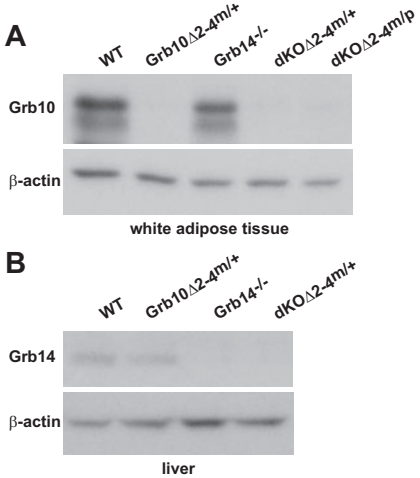

FIG. 1. Grb10 and Grb14 protein expression is ablated in double-knockout mice. A, White adipose tissue was analyzed by Western blotting for the expression of Grb10. Samples from both dKOΔ2-4$^{m/+}$ and dKOΔ2-4$^{m/p}$ mice are shown for comparative purposes. In the latter, both Grb10 alleles are disrupted. B, Liver was analyzed by Western blotting for the expression of Grb14. Expression of β-actin was used to verify equal loading in each case.

We have previously shown that adult mice with a disruption to the Grb10 gene have an increase in total body weight (14). To investigate the effect of ablating the Grb10 and Grb14 genes in combination, we first examined body weights of mice at 6 months of age. Consistent with our earlier work, Grb10Δ2-4$^{m/+}$ mice were 15% heavier than their wild-type (WT) counterparts (Fig. 2A). This weight differential was maintained in the dKOΔ2-4$^{m/+}$ mice. Previously we reported that the weight phenotype of Grb10Δ2-4$^{m/+}$ mice is accounted for by an increase in lean mass (14). Therefore, to determine whether lean mass contributed to the increased body weight of dKOΔ2-4$^{m/+}$ mice, we undertook a dual-energy x-ray absorptiometry (DXA) analysis of body composition. We found that dKOΔ2-4$^{m/+}$ mice had a similar increase in lean mass to Grb10Δ2-4$^{m/+}$ mice (Fig. 2A). When the lean mass was expressed as a percentage of total body weight, the difference was normalized, suggesting that increased lean mass explained the enhanced body weight of these animals. The lean mass measured by DXA predominantly represents muscle mass. To investigate the lean phenotype in more detail, we dissected out the tibialis anterior muscles and analyzed their weights. Consistent with our previous study (14), the tibialis muscle was significantly larger in Grb10Δ2-4$^{m/+}$ mice (Fig. 2B). The increase in tibialis weight was also significantly different in the double-knockout mice. In our previous study, Grb10Δ2-4$^{m/+}$ animals exhibited a significant reduction in adiposity (14). This effect was less evident on the altered genetic background used in this study, as determined by both DXA (Fig. 2A) and direct weighing of the epididymal depot (Fig. 2C), but the double-knockout animals also exhibited a trend for decreased adipose tissue. Several other tissues (heart, kidney, liver, spleen) were not significantly different in size between genotypes. However, the pancreas was larger in both Grb10Δ2-4$^{m/+}$ and dKOΔ2-4$^{m/+}$ mice (Fig. 2C). Ablation of Grb14 did not affect animal weight or body composition (Fig. 2). Overall, these data indicate that the lean phenotype of Grb10Δ2-4$^{m/+}$ mice is maintained in dKOΔ2-4$^{m/+}$ animals.

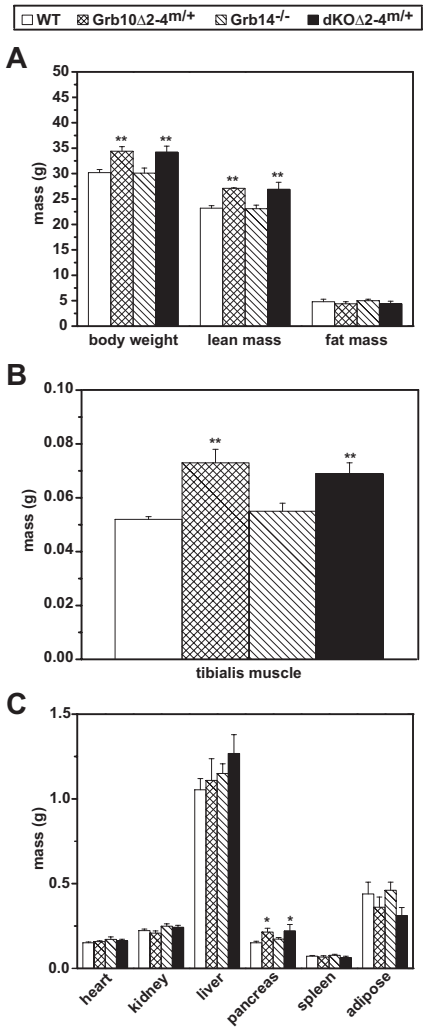

FIG. 2. dKOΔ2-4$^{m/+}$ mice have increased body weight and altered body composition. A, Body weights of 6-month-old mice fed a chow diet and values for their lean and fat mass, determined by DXA analysis. B, Dissected weight for tibialis anterior muscle and (C) tissue weights. Values are expressed as means ± SEM; n = 4–7 mice per group for body weight, n = 4–9 for tissue weights. *, $P < 0.05$; **, $P < 0.01$ relative to WT by Fisher's PLSD test.

Effect of high-fat diet (HFD) on body weight and body composition

To determine how a HFD affects body composition in mice of the different genotypes, mice were fed a specialized diet, providing 45% of calories from fat, for 16 wk beginning at 8 wk of age. DXA analysis revealed that mice of all genotypes displayed a significant increase in fat mass on a HFD (Fig. 3A). Interestingly, this effect was significantly enhanced in Grb14$^{-/-}$ animals. Examination of epididymal adipose depots revealed that fat-fed Grb10Δ2-4$^{m/+}$ and dKOΔ2-4$^{m/+}$ mice had significantly less fat at these sites than either WT or Grb14$^{-/-}$ mice (Fig. 3B). In the case of Grb14-deficient animals, the increase in fat mass detected by DXA (Fig. 3A) was not accompanied by a parallel increase in epididymal fat mass (Fig. 3B). Consequently, either small differences in a number of adipose depots may result in a significant overall difference as measured by DXA or, alternatively, there may be depot-specific differences in fat accumulation, with no change observed for the epididymal depot. DXA analysis revealed that the increased lean mass exhibited by Grb10Δ2-4$^{m/+}$ and dKOΔ2-4$^{m/+}$ mice (Fig. 2A) was maintained after a HFD (Fig. 3C), and this was reflected in significantly increased tibialis muscle weights for both genotypes (Fig. 3D).

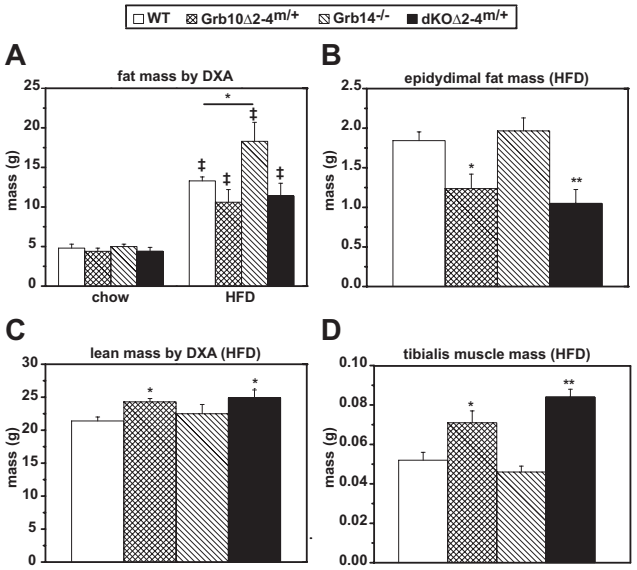

FIG. 3. Effect of HFD on body composition. Fat mass of 6-month-old mice fed a HFD, analyzed by DXA (A) or dissected epididymal fat mass (B). Lean mass of mice on a HFD analyzed by DXA (C) or dissected tibialis muscle mass (D). Values are expressed as means ± SEM; n = 4–9 mice/group. *, $P < 0.05$; **, $P < 0.01$ relative to WT on the same diet, by Fisher's PLSD test; ‡, $P < 0.05$ for comparison of chow with HFD for each genotype, by Fisher's PLSD test.

Insulin-induced signaling in compound gene knockout mice

To determine the combined roles of Grb10 and Grb14 in regulation of insulin signaling, we characterized the phosphorylation status of the IR, IRS-1, and Akt using phosphospecific antibodies against key regulatory sites. Phosphorylation of the IR activation loop on Y1162 and Y1163 is critical for kinase activation and downstream signaling (17), and Y612 of IRS-1 is a major site for p85 binding and hence PI3-kinase activation (18). In addition, we have previously demonstrated that increased phosphorylation of IRS-1 on this site upon Grb14 ablation correlates with enhanced IRS-1/p85 association (10). Finally, the kinase domain residue T308 is a major positive regulatory site in Akt (19). Our analysis was restricted to these sites so that the impact of all genotypes could be examined in a range of insulin-responsive tissues. However, we acknowledge that all three proteins are subject to phosphorylation on additional sites and other modes of regulation.

Grb10 and Grb14 are both expressed in quadriceps muscle and white adipose tissue (10, 14, 15). In the former tissue, and for chow-fed animals, ablation of neither adaptor alone altered IR expression. However, total IR levels were significantly increased in the double knockouts, indicating redundant roles for Grb10 and Grb14 in negative regulation of IR expression (Figs. 4 and 5A). Consistent with our previous findings (10, 14), Grb10Δ2-$4^{m/+}$, but not Grb$14^{-/-}$, animals exhibited IR

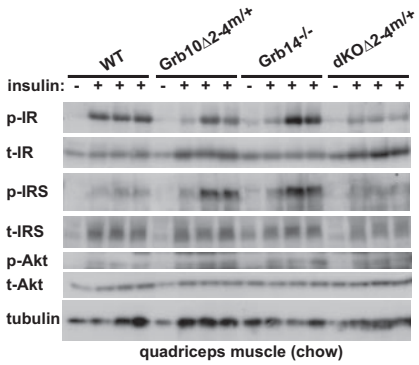

FIG. 4. Insulin-induced signaling in quadriceps muscle of gene knockout mice. Chow-fed mice were anesthetized at 6 months of age and then injected with (+) or without (−) insulin (1 U/kg) via the inferior vena cava. After 2 min, quadriceps muscle was collected and immediately frozen in liquid nitrogen. Solubilized muscle samples were subjected to Western blotting as indicated. Representative Western blots are shown.p-IR, Phosphorylated IR; t-IR, total IR.

hypophosphorylation in quadriceps muscle (Figs. 4 and 5C). However, evidence that Grb14 can contribute to regulation of muscle IR phosphorylation was obtained by analysis of animals on a HFD, in which the individual knockouts were without effect, but there was marked receptor hypophosphorylation in dKOΔ2-$4^{m/+}$ mice (Fig. 5D) despite normal IR levels (Fig. 5B). Total IRS-1 levels were similar in quadriceps muscles from chow-fed animals of all genotypes (Figs. 4 and 6A). However, IRS-1

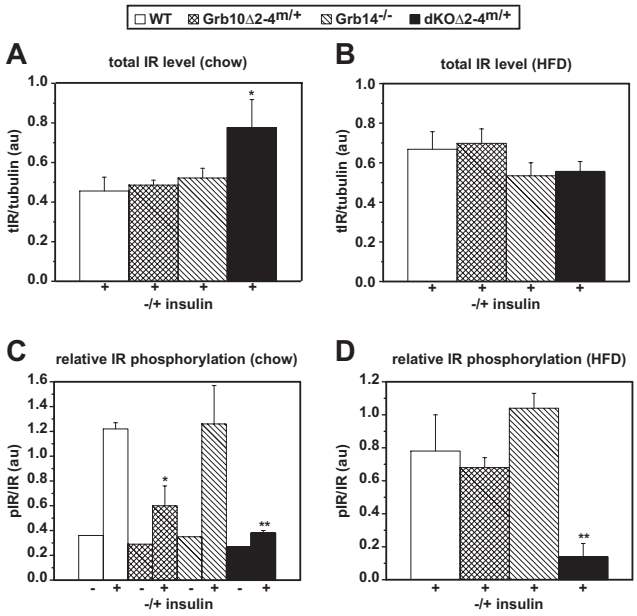

FIG. 5. Insulin-induced signaling to IR in quadriceps muscle of mice fed a chow or HFD. Western blots were quantified by densitometry. Total IR normalized for tubulin in (A) chow-fed mice and (B) HFD-fed mice. The phosphorylated signal for IR was adjusted for its total level to give a measurement of phosphorylated IR in (C) chow-fed mice and (D) HFD-fed mice. Values for insulin-stimulated samples are expressed as means ± SEM; n = 1 (−insulin), n = 3–4 (+insulin). *, $P < 0.05$; **, $P < 0.01$ relative to WT on the same diet, by Fisher's PLSD test. pIR, Phosphorylated IR; tIR, total IR; au, arbitrary units.

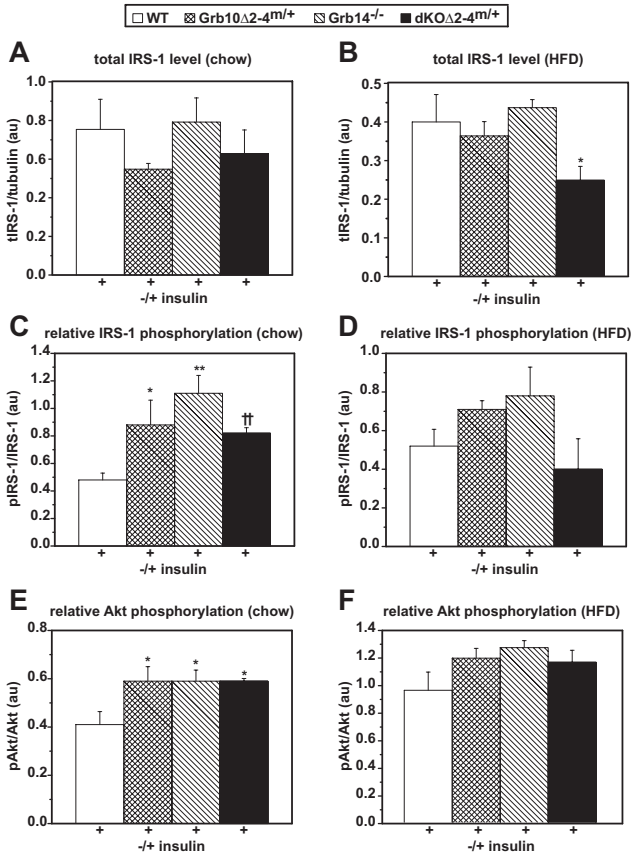

FIG. 6. Insulin-induced signaling to IRS-1 and Akt in quadriceps muscle of mice fed a chow or HFD. Western blots were quantified by densitometry. Total IRS-1 normalized for tubulin in (A) chow-fed mice and (B) HFD-fed mice. The phosphorylated signal for each protein was adjusted for its total level to give a measurement of phosphorylated IRS-1 in (C) chow-fed mice and (D) HFD-fed mice and phosphorylated Akt in (E) chow-fed mice and (F) HFD-fed mice. Values for insulin-stimulated samples are expressed as means ± SEM; n = 3 (chow), n = 4 (HFD). *, $P < 0.05$; **, $P < 0.01$ relative to WT on the same diet, by Fisher's PLSD test; ††, $P < 0.01$ relative to WT on the same diet, by Student's *t* test. pIRS, Phosphorylated IRS; tIRS, total IRS; au, arbitrary units.

expression was significantly reduced in fat-fed dKOΔ2-4$^{m/+}$ animals (Fig. 6B). Characterization of insulin-induced IRS-1 tyrosine phosphorylation revealed a significant enhancement in quadriceps muscle of chow-fed Grb10Δ2-4$^{m/+}$ and Grb14$^{-/-}$ animals, as previously reported (10, 14), whereas in dKOΔ2-4$^{m/+}$ mice, IRS-1 tyrosine phosphorylation was also increased, but only to a level comparable to that in the single knockouts (Figs. 4 and 6C). These effects on IRS-1 in the knockout animals were paralleled by corresponding changes in phosphorylation of the downstream effector Akt on T308 (Figs. 4 and 6E). For animals on a HFD, signaling to IRS-1 was similar in the double knockouts relative to WT controls (Fig. 6D). In line with this, Akt phosphorylation was comparable in WT and dKOΔ2-4$^{m/+}$ mice (Fig. 6F). In white adipose tissue, for animals on either a chow diet or HFD, dual ablation of Grb10 and Grb14 did not lead to further enhancement of IRS-1 phosphorylation or Akt activation relative to the individual knockouts (data not shown).

Grb14 is expressed at high levels in adult liver, whereas Grb10 levels are reportedly low (14, 15, 20). Ablation of Grb10 and Grb14, alone or in combination, did not lead to marked changes in IR expression for chow- or fat-fed animals (data not shown). In line with previous findings, the IR was significantly hypophosphorylated in liver from chow-fed Grb14$^{-/-}$ animals (Fig. 7A). However, Grb10 ablation also led to reduced IR phosphorylation, and an additive effect was observed in the double knockouts, so that IR phosphorylation in dKOΔ2-4$^{m/+}$ mice was significantly less than in Grb14$^{-/-}$ animals (Fig. 7A). Significant receptor hypophosphorylation was also observed for double-knockout animals on a HFD (Fig. 7B). Consequently, on this genetic background, Grb10 does contribute to regulation of liver IR phosphorylation. Interest-

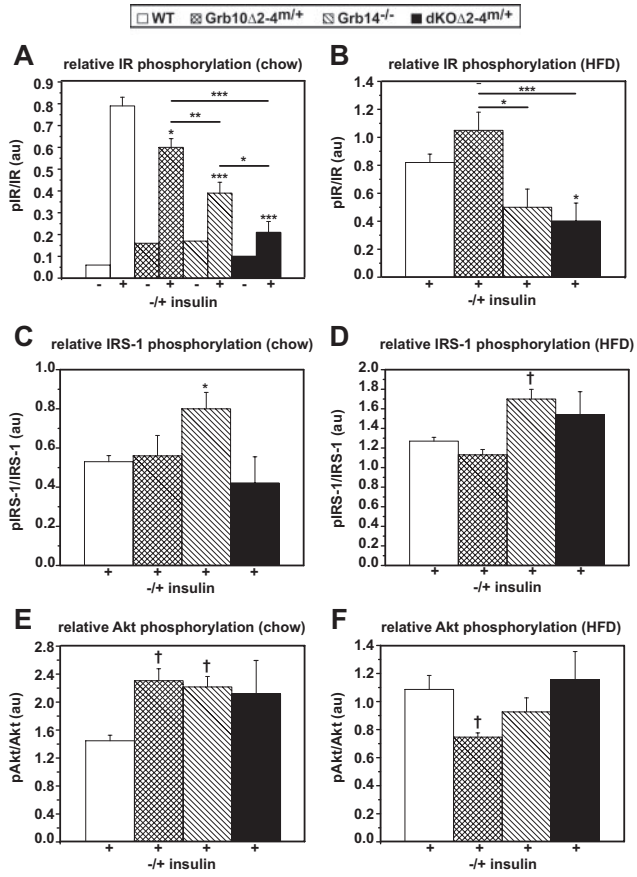

FIG. 7. Insulin-induced signaling in liver of mice fed a chow or HFD. Western blots were quantified by densitometry, and the phosphorylated signal for each protein was adjusted for its total level to give a measurement of phosphorylated IR in (A) chow-fed mice and (B) HFD-fed mice, phosphorylated IRS-1 in (C) chow-fed mice and (D) HFD-fed mice, and phosphorylated Akt in (E) chow-fed mice and (F) HFD-fed mice. Values for insulin-stimulated samples are expressed as means ± SEM; n = 1 (−insulin), n = 3 (+insulin, chow), n = 3–4 (+insulin, HFD). *, $P < 0.05$; **, $P < 0.01$; ***, $P < 0.001$ relative to WT (unless otherwise indicated) on the same diet, by Fisher's PLSD test; †, $P < 0.05$ relative to WT on the same diet, by Student's *t* test. pIR, Phosphorylated IR; pIRS, phosphorylated IRS; au, arbitrary units.

ingly, the effects of the different knockouts on IRS-1 expression in liver were similar to those observed in muscle: no effects for chow-fed animals of any knockout genotype, but a significant, approximately 2-fold reduction in IRS-1 expression for fat-fed dKOΔ2-4$^{m/+}$ mice ($P < 0.05$ by ANOVA with Fisher's protected least significant difference (PLSD) test; data not shown). Consistent with our previous study (9), IRS-1 tyrosine phosphorylation was significantly increased in the livers of chow-fed Grb14$^{-/-}$ mice (Fig. 7C). This effect was also observed in fat-fed animals (Fig. 7D) but was not evident in Grb10Δ2-4$^{m/+}$ mice on either diet. For dKOΔ2-4$^{m/+}$ animals on a chow or HFD, IRS-1 tyrosine phosphorylation was similar to WT controls (Fig. 7, C and D). For chow-fed animals, a significant enhancement of Akt phosphorylation in liver was observed in both Grb10- and Grb14-deficient mice, but in line with data from muscle, an additive effect was not detected in double-knockout mice (Fig. 7E). For animals on a HFD, Akt activation in liver was reduced in Grb10Δ2-4$^{m/+}$ mice and comparable to WT animals for the other genotypes (Fig. 7F).

Overall, these data indicate that although ablation of either Grb10 or Grb14 can enhance insulin-induced signaling, this is not increased further upon their combined loss, and under certain conditions, may be attenuated by the IR hypophosphorylation and/or decreased IRS-1 expression that occurs.

Effect of compound disruption of Grb10 and Grb14 on whole-body glucose homeostasis

We have previously demonstrated that both the Grb10 and Grb14 knockout mouse models have improved whole-body glucose homeostasis (10, 14). To determine whether compound gene disruption enhanced this effect, we performed glucose tolerance tests on dKOΔ2-4$^{m/+}$ mice. Whereas the fasting blood glucose levels of chow-fed mice of all genotypes were similar (Table 1), the glucose tolerance of Grb14$^{-/-}$ and double-knockout mice was significantly improved compared with WT animals (Fig. 8, A and B). In addition, we performed glucose tolerance tests on mice that had been fed a HFD for 16 wk. Whereas ablation of Grb10 and Grb14 alone, or in combination, prevented HFD-induced hyperinsulinemia (Table 1), neither of the single-gene disruptions affected the impaired glucose tolerance that results from high-fat feeding (Fig. 8, A and B). In contrast, the incremental area under the glucose tolerance curve for dKOΔ2-4$^{m/+}$ mice on the HFD was similar to WT mice on chow diet (incremental area under the curve = 965 and 955, respectively; $P = 0.9$ by ANOVA with Fisher's PLSD test), indicating that dual ablation of Grb10 and Grb14 allows maintenance of normal glucose homeostasis following this dietary regimen (Fig. 8B).

TABLE 1. Plasma concentrations of glucose and insulin in fasted mice

Genotype	Chow diet	HFD
Glucose (mM)		
WT	8.0 ± 0.3	11.0 ± 0.5
Grb10Δ2-4$^{m/+}$	7.8 ± 0.3	9.3 ± 0.7
Grb14$^{-/-}$	8.8 ± 0.3	10.5 ± 0.5
dKOΔ2-4$^{m/+}$	8.1 ± 0.2	10.0 ± 0.9
Insulin (ng/ml)		
WT	0.84 ± 0.14	1.36 ± 0.18[a]
Grb10Δ2-4$^{m/+}$	0.98 ± 0.18	0.52 ± 0.27[b]
Grb14$^{-/-}$	0.61 ± 0.09	0.79 ± 0.11[c]
dKOΔ2-4$^{m/+}$	0.78 ± 0.15	0.57 ± 0.15[c]

Data are presented as means ± SEM (n = 3–12 mice per group): [a], $P < 0.05$ for chow *vs.* HFD-fed mice, by Fisher's PLSD test; [b] $P < 0.01$ relative to WT on the same diet; [c], $P < 0.05$.

Discussion

In recent years, it has become evident that, in addition to the canonical IR targets IRS-1/2 and Shc, several adaptor-type signaling proteins bind directly to the IR in an insulin-dependent manner and regulate signal output. In the case of SH2-B, this results in amplification of IR signaling (21). In contrast, Grb10 and Grb14 perform a negative modulatory role (9, 10, 14). However, how these adap-

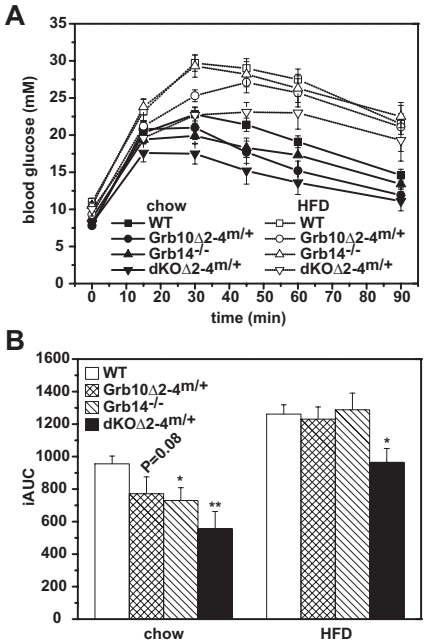

FIG. 8. Compound disruption of Grb10 and Grb14 protects against HFD-induced glucose intolerance. A, Glucose tolerance tests for 6 month-old mice fed either chow or HFD. B, Quantification of the incremental area under the curve for total glycemic excursions from panel A. Values are expressed as means ± SEM; n = 4–13 mice per group. *, $P < 0.05$; **, $P < 0.01$ relative to WT on the same diet, by Fisher's PLSD test. IAUC, Incremental area under the curve.

tors cooperate to regulate insulin signaling and whole-body glucose metabolism remains poorly characterized.

In this study, we have used dual gene disruption to characterize, for the first time, the combined physiological roles of Grb10 and Grb14. Interestingly, whereas Grb14-deficient mice on a mixed 129/SvJ x C57BL/6 background exhibited a slight decrease in body weight (10), this was not observed on the different genetic background used in this study. However, the increases in body weight and lean mass that occur in Grb10Δ2-4$^{m/+}$ mice (14) were largely phenocopied in dKOΔ2-4$^{m/+}$ animals, indicating that these effects represent a functional role of Grb10 that is not shared by Grb14. The enhanced body weight of Grb10-deficient adult mice reflects the ability of Grb10 to suppress fetal growth. This may be mediated via a pathway outside of the IGF axis, because it is independent of IGF-II (16). However, disruption to negative regulation of the IGF-1 receptor by Grb10 (22) may lead to postnatal maintenance of increased muscle mass in Grb10-deficient animals (14). Whether Grb14 also regulates the IGF-1 receptor is unclear at present, although the phenotype of Grb14$^{-/-}$ mice suggests that this adaptor may be more specific for the IR. Consequently, it will be of great interest to further characterize the growth-regulatory pathway(s) modulated by Grb10 and to identify the structural determinants that confer signaling specificity to Grb10 and Grb14.

Our previous studies determined that upon Grb10 or Grb14 ablation, enhanced signaling to IRS-1 can occur in particular tissues despite relative IR hypophosphorylation (10, 14). This may reflect the increased catalytic activity of the residual phosphorylated receptor due to the absence of a pseudosubstrate inhibitor (9), and/or spatiotemporal segregation of signaling events, so that receptor coupling to IRS-1 occurs at the plasma membrane and before receptor dephosphorylation, which occurs after internalization (23). However, although under certain conditions IR hypophosphorylation is increased in dKOΔ2-4$^{m/+}$ mice compared with Grb10Δ2-4$^{m/+}$ or Grb14$^{-/-}$ animals (Figs. 5D and 7A), it is not paralleled by a further enhancement of signaling to IRS-1. Instead, signaling is similar to that observed in WT animals (Figs. 6D and 7C). A potential explanation is that Grb10 and Grb14, while gating the initial signal output from the receptor, perform an additional role of maintaining a pool of receptor in a latent, but activated, state, as discussed by Dufresne and Smith (22). Because the IR-adaptor association is presumably dynamic, cycles of disassociation/association of the adaptor with the receptor may then allow maintenance of IRS-1 phosphorylation, while protecting the receptor from PTP activity. This explains the apparent conundrum of Grb10 and Grb14 performing two opposing roles in inhibiting the catalytic activity of the receptor, but protecting it from dephosphorylation. It is also consistent with a recent report that IR-Grb14 complexes can be detected in the endosomal fraction of rat liver (24). According to our model, ablation of one adaptor results in enhanced signaling to IRS-1 at the plasma membrane, but to maintain this level of IRS-1 tyrosine phosphorylation, a pool of receptor must be protected from dephosphorylation after internalization and remain in an active state. This protective function can be provided by the remaining adaptor in the single knockouts. However, in the double knockouts, the enhanced receptor dephosphorylation results in there being insufficient activated IR to maintain sustained IRS-1 tyrosine phosphorylation.

This study has also revealed effects of dual Grb10/14 deficiency on the expression levels of two components of the insulin-signaling network. Previously we reported that Grb10 ablation led to increased IR levels in quadriceps muscle of chow-fed animals (14). However, on the modified genetic background used in the double-knockout study, this effect was only observed for dKOΔ2-4$^{m/+}$ mice (Fig. 5A). Although the ability of Grb10 to promote IR degradation has been reported (25), this is the first indication that Grb14 also contributes to this process. Second, IRS-1 expression was significantly reduced in muscle and liver of fat-fed double-knockout animals. Because this represents a novel effect of Grb10 or Grb14, it will be important to determine the level at which this regulation occurs. Of note, it has recently been reported that the CUL7 E3 ubiquitin ligase targets the IRS-1 docking protein for ubiquitin-dependent degradation after mammalian target of rapamycin-dependent phosphorylation of IRS-1 (4). Consequently, one possibility is that the absence of Grb10 and Grb14 leads to enhanced phosphorylation of IRS-1 by particular serine/threonine kinases, leading to its degradation. This is currently under investigation.

As well as characterizing the effects of combined Grb10 and Grb14 deletion on insulin signaling, this study provides a significant insight into the physiological significance of global deletion of these genes on glucose homeostasis. Because the double-knockout animals exhibited protection from the impaired glucose tolerance that results from high-fat feeding, this indicates that the gene deletions are having nonredundant effects that, when combined, can significantly alter the way the animal disposes of a glucose load. However, although the muscle phenotype of Grb10Δ2-4$^{m/+}$ animals is maintained in the double knockout, enhanced signaling to Akt in insulin-responsive tissues, relative to the single knockouts, is not readily apparent. A potential explanation is that the en-

hancement of Akt activation upon Grb10 and Grb14 ablation is masked at high insulin concentrations, as previously reported for mice with peripheral disruption of Grb10 (15). Alternatively, Grb10 and Grb14 may have additional functions that impact upon glucose homeostasis, beyond their known roles in regulating coupling of the IR to IRS-1. Indeed, it was recently reported that Grb14 plays a positive role in promoting sterol regulatory element-binding protein 1c maturation in primary hepatocytes (26), although this cannot explain the improved glucose homeostasis of the double-knockout animals. Finally, the effects of combined Grb10 and Grb14 ablation on whole body glucose homeostasis may be indirect, and reflect, for example, altered cross talk between muscle and liver. Irrespective of the underlying mechanism, this study provides strong evidence that these two adaptors represent potential therapeutic targets for treatment of insulin-resistant states.

Materials and Methods

Animal maintenance

Animals were kept on a 12-h light, 12-h dark cycle with free access to food and water. They were fed either a standard laboratory chow diet, or a HFD (45% of calories from fat, 35% of calories from carbohydrate, and 20% of calories from protein) for 16 wk, beginning at 8 wk of age. All experiments were carried out on male mice and were undertaken with the approval of the Garvan Institute/St Vincent's Hospital Animal Ethics Committee, following guidelines issued by the National Health and Medical Research Council of Australia. Animal weights and food intake were monitored weekly.

Metabolic assays

Glucose tolerance tests (2 g/kg glucose ip) were performed on overnight-fasted (~16 h) mice that were matched for age. Blood samples were obtained from the tail tip to measure the glucose levels at the appropriate timepoint using a glucometer (Accu-Check II; Roche, Indianapolis, IN). For plasma measurements, blood was collected after euthanasia from the chest cavity and then centrifuged at 13,000 rpm for 10 min to obtain the plasma. Plasma insulin concentrations were assayed using a commercial RIA kit (Linco Research, Inc., St. Charles, MO).

Determination of body composition

Lean and fat body masses were measured using DXA (Lunar PIXImus2 mouse densitometer; GE Healthcare, Piscataway, NJ) according to the manufacturer's instructions.

Insulin signaling studies and Western blot analysis

Overnight-fasted mice were anesthetized with pentobarbital sodium (30 mg/kg) after which insulin (1 U/kg) was injected into the inferior vena cava. After 2 min, liver, white adipose tissue, quadriceps muscle, and tibialis muscle were collected and immediately frozen in liquid nitrogen. The tissues were solubilized (after powdering in the case of muscle) for 2 h at 4 C in modified RIPA buffer (65 mM Tris; 150 mM NaCl; 5 mM EDTA; 0.1% Nonidet P-40; 0.5% sodium deoxycholate; 0.1% sodium dodecyl sulfate; 10% glycerol, pH 7.4) supplemented with protease and phosphatase inhibitors (10 μg/μl aprotinin, 10 μg/μl leupeptin, 20 mM NaF, 1 mM Na orthovanadate, 1 mM phenylmethylsulfonyl fluoride). Cleared tissue lysates were resolved by SDS-PAGE and immunoblotted with antibodies against Grb10 (a kind gift from Prof. Feng Liu, University of Texas Health Science Center at San Antonio, San Antonio, TX) (15), Grb14 (Chemicon, Temecula, CA), the IR β-subunit (BD Transduction Laboratories, Lexington, KY), phospho-IR (pY1162/3; Biosource, San Jose, CA), IRS-1 (Upstate Biotechnology, Inc., Santa Cruz, CA), phospho IRS-1/2 (pY612, Biosource), Akt or phospho Akt (pT308) (both from Cell Signaling Technology, Danvers, MA), β-tubulin (Amersham Pharmacia Biotech, Piscataway, NJ) or β-actin (Sigma, St. Louis, MO). Quantitation of immunolabeled bands was performed using IP Lab Gel H (BD Biosciences).

Statistical analysis

Data are presented as mean ± SEM. Statistical analysis of all data was performed using ANOVA with a Fisher's PLSD *post hoc* test. For additional analysis of individual comparisons, unpaired Student's *t* tests were performed as indicated in the figure legends. Differences at $P < 0.05$ were considered to be statistically significant.

Acknowledgments

Address all correspondence and requests for reprints to: Roger J. Daly, Cancer Research Program, Garvan Institute of Medical Research, 384 Victoria Street, Darlinghurst, Sydney, New South Wales 2010, Australia. E-mail: r.daly@garvan.org.au.

This work was supported by research grants (to R.J.D. and G.J.C.) from the National Health and Medical Research Council of Australia; and by the UK Biotechnology and Biological Sciences Research Council and Medical Research Council (to A.W.).

Disclosure Summary: The authors have nothing to disclose.

References

1. **Saltiel AR, Kahn CR** 2001 Insulin signalling and the regulation of glucose and lipid metabolism. Nature 414:799–806
2. **Saltiel AR** 2001 New perspectives into the molecular pathogenesis and treatment of type 2 diabetes. Cell 104:517–529
3. **Taniguchi CM, Emanuelli B, Kahn CR** 2006 Critical nodes in signalling pathways: insights into insulin action. Nat Rev 7:85–96
4. **Xu X, Sarikas A, Dias-Santagata DC, Dolios G, Lafontant PJ, Tsai SC, Zhu W, Nakajima H, Nakajima HO, Field LJ, Wang R, Pan ZQ** 2008 The CUL7 E3 ubiquitin ligase targets insulin receptor substrate 1 for ubiquitin-dependent degradation. Mol Cell 30:403–414
5. **Elchebly M, Payette P, Michaliszyn E, Cromlish W, Collins S, Loy AL, Normandin D, Cheng A, Himms-Hagen J, Chan CC, Ramachandran C, Gresser MJ, Tremblay ML, Kennedy BP** 1999 Increased insulin sensitivity and obesity resistance in mice lacking the protein tyrosine phosphatase-1B gene. Science 283:1544–1548
6. **Gum RJ, Gaede LL, Koterski SL, Heindel M, Clampit JE, Zinker BA, Trevillyan JM, Ulrich RG, Jirousek MR, Rondinone CM** 2003 Reduction of protein tyrosine phosphatase 1B increases insulin-dependent signaling in ob/ob mice. Diabetes 52:21–28
7. **Holt LJ, Daly RJ** 2005 Adapter protein connections: the MRL and Grb7 protein families. Growth Factors 23:193–201

8. **Holt LJ, Siddle K** 2005 Grb10 and Grb14: enigmatic regulators of insulin action—and more? Biochem J 388:393–406
9. **Depetris RS, Hu J, Gimpelevich I, Holt LJ, Daly RJ, Hubbard SR** 2005 Structural basis for inhibition of the insulin receptor by the adaptor protein Grb14. Mol Cell 20:325–333
10. **Cooney GJ, Lyons RJ, Crew AJ, Jensen TE, Molero JC, Mitchell CJ, Biden TJ, Ormandy CJ, James DE, Daly RJ** 2004 Improved glucose homeostasis and enhanced insulin signalling in Grb14-deficient mice. EMBO J 23:582–593
11. **Béréziat V, Kasus-Jacobi A, Perdereau D, Cariou B, Girard J, Burnol AF** 2002 Inhibition of insulin receptor catalytic activity by the molecular adapter Grb14. J Biol Chem 277:4845–4852
12. **Nouaille S, Blanquart C, Zilberfarb V, Boute N, Perdereau D, Roix J, Burnol AF, Issad T** 2006 Interaction with Grb14 results in site-specific regulation of tyrosine phosphorylation of the insulin receptor. EMBO Rep 7:512–518
13. **Cariou B, Capitaine N, Le Marcis V, Vega N, Béréziat V, Kergoat M, Laville M, Girard J, Vidal H, Burnol AF** 2004 Increased adipose tissue expression of Grb14 in several models of insulin resistance. FASEB J 18:965–967
14. **Smith FM, Holt LJ, Garfield AS, Charalambous M, Koumanov F, Perry M, Bazzani R, Sheardown SA, Hegarty BD, Lyons RJ, Cooney GJ, Daly RJ, Ward A** 2007 Mice with a disruption of the imprinted Grb10 gene exhibit altered body composition, glucose homeostasis, and insulin signaling during postnatal life. Mol Cell Biol 27:5871–5886
15. **Wang L, Balas B, Christ-Roberts CY, Kim RY, Ramos FJ, Kikani CK, Li C, Deng C, Reyna S, Musi N, Dong LQ, DeFronzo RA, Liu F** 2007 Peripheral disruption of the Grb10 gene enhances insulin signaling and sensitivity in vivo. Mol Cell Biol 27:6497–6505
16. **Charalambous M, Smith FM, Bennett WR, Crew TE, Mackenzie F, Ward A** 2003 Disruption of the imprinted Grb10 gene leads to disproportionate overgrowth by an Igf2-independent mechanism. Proc Natl Acad Sci USA 100:8292–8297
17. **Hubbard SR** 1997 Crystal structure of the activated insulin receptor tyrosine kinase in complex with peptide substrate and ATP analog. EMBO J 16:5572–5581
18. **Esposito DL, Li Y, Cama A, Quon MJ** 2001 Tyr(612) and Tyr(632) in human insulin receptor substrate-1 are important for full activation of insulin-stimulated phosphatidylinositol 3-kinase activity and translocation of GLUT4 in adipose cells. Endocrinology 142:2833–2840
19. **Franke TF** 2008 PI3K/Akt: getting it right matters. Oncogene 27:6473–6488
20. **Laviola L, Giorgino F, Chow JC, Baquero JA, Hansen H, Ooi J, Zhu J, Riedel H, Smith RJ** 1997 The adapter protein Grb10 associates preferentially with the insulin receptor as compared with the IGF-I receptor in mouse fibroblasts. J Clin Invest 99:830–837
21. **Duan C, Yang H, White MF, Rui L** 2004 Disruption of the SH2-B gene causes age-dependent insulin resistance and glucose intolerance. Mol Cell Biol 24:7435–7443
22. **Dufresne AM, Smith RJ** 2005 The adapter protein GRB10 is an endogenous negative regulator of insulin-like growth factor signaling. Endocrinology 146:4399–4409
23. **Asante-Appiah E, Kennedy BP** 2003 Protein tyrosine phosphatases: the quest for negative regulators of insulin action. Am J Physiol 284:E663–E670
24. **Desbuquois B, Béréziat V, Authier F, Girard J, Burnol AF** 2008 Compartmentalization and in vivo insulin-induced translocation of the insulin-signaling inhibitor Grb14 in rat liver. FEBS J 275:4363–4377
25. **Ramos FJ, Langlais PR, Hu D, Dong LQ, Liu F** 2006 Grb10 mediates insulin-stimulated degradation of the insulin receptor: a mechanism of negative regulation. Am J Physiol 290:E1262–E1266
26. **Carré N, Caüzac M, Girard J, Burnol AF** 2008 Dual effect of the adapter growth factor receptor-bound protein 14 (grb14) on insulin action in primary hepatocytes. Endocrinology 149:3109–3117